Pressure-Dependent Elasticity and Energy Conservation in Elastoplastic Models for Soils

Itai Einav[1] and Alexander M. Puzrin, A.M.ASCE[2]

Abstract: This paper presents a study on the consequences of combining energy conservative or non-conservative elasticity within a plasticity framework. Toward this end, a versatile energy potential function is first presented and examined. It is shown to cover a wide range of existing empirical relations for pressure-dependent stiffness of soils. Utilization of these functions within hyperplastic constitutive framework allows for the resulting models to satisfy the Law of Energy Conservation for both elastic and plastic components of soil behavior. Apart from the theoretical rigor, a very important result of this approach is that it automatically implies stress-induced cross-anisotropy of the elastic component of soil behavior and dilatancy term occurs due to shear modulus dependency on pressure. Proper modeling of these phenomena, normally neglected by conventional hypoelastic-plastic models, has been shown to have a significant effect on the accuracy of the model predictions of undrained behavior of overconsolidated clays both in laboratory tests and in tunnel excavation problem.

DOI: 10.1061/(ASCE)1090-0241(2004)130:1(81)

CE Database subject headings: Constitutive relations; Elasticity; Energy conservation; Elastoplasticity; Anisotropy; Tunneling.

Introduction

Elastoplastic constitutive modeling is significantly influenced by the elasticity component of its formulation. Unlike metals, elastic properties of soils are widely accepted to be greatly dependent on the mechanical state variables. In the critical state family of models, for instance, the elastic bulk modulus is usually assumed to be linear pressure dependent, while the shear modulus is either constant or linear pressure dependent for constant Poisson's ratio. Generally, constant Poisson's ratio, used in connection with the variable bulk modulus, results in a pressure-dependent shear modulus. The later is commonly incorporated into elastoplastic constitutive models using hypoelastic formulation (Truesdell 1965). However, implementation of the hypoelastic formulation to the case of nonlinear elastic soil response could produce nonconservative models in terms of energy conservation (Ko and Masson 1976; Zytynski et al. 1978). The importance of treating elastic behavior in a rigorous and thermomechaniclly consistent manner was both theoretically emphasized (Ko and Masson 1976; Houlsby 1985; Hueckel et al. 1992) and numerically studied (Borja et al. 1997). However, for geotechnical engineering purposes, it is even more important to attempt an assessment of the effects, which violation of the energy conservation may have on solution of geotechnical boundary value problems; this is the main objective of the present paper.

An alternative to hypoelastic approach is hyperelasticity, which even for nonlinear pressure-dependent elastic moduli always results in energy conservative models. However, this approach leads to coupling between volumetric and deviatoric stress-strain behavior, i.e., the material behavior is modeled as elastic with stress-induced cross-anisotropy, and additional dilatancy term. In fact, there is extensive experimental evidence (Lo Presti and O'Neill 1991; Stokoe et al. 1991; Hoque and Tatsuoka 1998) confirming stress-induced cross-anisotropy phenomenon in soils. While some researchers recognized this phenomenon and developed a consistent formulation (Houlsby 1985; Hueckel et al. 1992; Borja et al. 1997), others tried to avoid this anisotropy by suggesting models with shear modulus being dependent on preconsolidation pressure instead of the current pressure (Houlsby 1981; Hashiguchi and Collins 2001). However, though the volumetric-deviatoric coupling is avoided by this formulation, it produces another kind of coupling: between elastic and plastic components of stress-strain behavior, i.e., the elastic properties depend on the plastic deformation. In this type of model, the assumption that the strain tensor can be decomposed into elastic and plastic components is not valid anymore and special care must be given to the precise definition of the ''elastic'' and ''plastic'' components of strains [see Maier and Hueckel (1977) and discussion by Einav and Puzrin (2002)]. As may be expected, the thermodynamic restrictions on materials with elastoplastic coupling are rather more complex in this formulation. We believe that a loss of strain decomposition assumption is too much of a sacrifice in order to avoid stress-induced cross-anisotropy, which in fact is exhibited by many soils. Therefore, the approach suggested by Houlsby (1985) and Borja et al. (1997) will be followed here in general. However, the particular hyperelastic stress-strain laws suggested in this previous work have rather limited versatility in description of real soil behavior. Therefore, another important objective of this paper is to present a versatile energy potential func-

[1]Research Associate, Univ. of Western Australia, Centre for Offshore Foundation Systems, 35 S Stirling Highway, Crawley Perth 6009, W. Australia (corresponding author); formerly, Israel Institute of Technology. E-mail: einav@cyllene.uwa.edu.au

[2]Associate Professor, School of Civil and Environmental Engineering, Georgia Institute of Technology, Atlanta, GA 30332; formerly, Israel Institute of Technology.

Note. Discussion open until June 1, 2004. Separate discussions must be submitted for individual papers. To extend the closing date by one month, a written request must be filed with the ASCE Managing Editor. The manuscript for this paper was submitted for review and possible publication on February 5, 2002; approved on February 22, 2003. This paper is part of the ***Journal of Geotechnical and Geoenvironmental Engineering***, Vol. 130, No. 1, January 1, 2004. ©ASCE, ISSN 1090-0241/2004/1-81–92/$18.00.

tion allowing for more realistic modeling of the elastic component of soil behavior.

In a boundary value problem (in the following we will use the term BVP) no guarantee can be given that in all points of continuum the stress-strain behavior will remain within the elastic range. Therefore, though our study is limited to comparison between performances of hypo- and hyperelastic models, it cannot be performed without their incorporation into some elastoplastic framework. Borja et al. (1997) showed how the hyperelastic stored energy function proposed by Houlsby (1985) could be incorporated into conventional elastoplastic formulation. In this approach, while the stress state is inside the yield surface the model agrees with thermodynamics. However, when yielding occurs and dissipation takes place, no guarantee is given for obeying thermodynamic principles.

Recently, the formulation of hyperplasticity (Ziegler 1983; Collins and Houlsby 1997; Houlsby and Puzrin 2000), which is closely related to the works of Halphen and Nguyen (1975), Martin and Nappi (1990), and Maugin (1992), and the more advanced formulation of continuous hyperplasticity (Puzrin and Houlsby 2001a,b) have been proposed. An important feature of these formulations is that they satisfy the First and the Second Laws of Thermodynamics for both elastic and plastic components of stress-strain behavior. The entire constitutive response of an elastoplastic model can be derived from the specification of two scalar potential functions (in hyperplasticity) or functionals (in continuous hyperplasticity). The first is the energy potential function, and the second is the dissipation function, which is related to the yield surface (or field of yield surfaces in continuous hyperplasticity). It has been shown that when the energy potential function has a specific form, the Green hyperelasticity can be derived from it automatically. The hyperplasticity and the continuous hyperplasticity can also accommodate elastoplastic coupling and could be used where the elastic moduli are assumed to be preconsolidation pressure dependent, yet this feature is beyond the scope of this paper. Thus, hyperplasticity serves as a solid basis for incorporating hyperelastic behavior into plastic models and will be used here for development of a complete elastoplastic model. Performance of this model in solution of a BVP will be evaluated against a similar conventional hypoelastic-plastic model.

Thus, the purpose of this paper is

- To present a versatile energy potential function for hyperelastic models;
- To demonstrate how hyperelasticity can be implemented in elastoplastic models in a manner that automatically ensures that the laws of thermodynamics are always obeyed;
- To present a qualitative comparison between a resulting hyperplastic model and a similar conventional hypoelastic-plastic model which violates the laws of thermodynamics; and
- To present an estimation of how violation of the laws of thermodynamics influences the solution of boundary value problems.

It should also be noted that this is a first attempt to apply hyperplastic model in finite elements or finite differences (FD) codes.

Preliminaries

In the following, we shall formulate potential function expressions in terms of triaxial variables; strainlike triaxial variables are given by

$$\varepsilon_v=\varepsilon_{kk};\quad \varepsilon_s=\sqrt{\frac{2}{3}e_{ij}e_{ij}};\quad e_{ij}=\varepsilon_{ij}-\frac{1}{3}\varepsilon_v\delta_{ij} \tag{1}$$

where ε_{ij}=small strain tensor and δ_{ij}=Kronecker delta. Stress-like triaxial variables are given by

$$p=\frac{1}{3}\sigma_{kk};\quad q=\sqrt{\frac{3}{2}s_{ij}s_{ij}};\quad s_{ij}=\sigma_{ij}-p\delta_{ij} \tag{2}$$

where σ_{ij}=effective Cauchy stress tensor, and all stresses referred to are effective stresses.

The formulation of hyperelasticity is based upon the existence of stored energy function. One option to express the stored energy function is by using the elastic strain potential function (the Helmholtz free energy function), which is given in triaxial form by $f_e=f_e[\varepsilon_v,\varepsilon_s]$. Another option is to express the stored energy potential by the negative complementary elastic energy function (the Gibbs free energy function) $g_e=g_e[p,q]$. Note that we used the subscript e for f and g to distinguish them from hyperplastic potential functions. In order for an elastic material to satisfy the restrictions of thermodynamics, it is both necessary and sufficient that the elastic behavior can be derived by the differentiation of these energy potential functions. The relation between these two functions is formulated by the use of the Legendre transformation for a hyperelastic material; the transformation for the case of isothermal hyperelastic material at triaxial conditions can be expressed as

$$f_e[\varepsilon_v,\varepsilon_s]=g_e[p,q]+p\varepsilon_v+q\varepsilon_s \tag{3}$$

In principle, once one function is specified the other can be found, although for certain choices of the functions it may not be possible to express one or the other in terms of conventional expressions.

The full description of cross-anisotropic elastic material requires five independent parameters (Love 1927). However, Graham and Houlsby (1983) showed that only three independent parameters could be extracted from conventional triaxial apparatus. In this case they suggested using the following relation:

$$\begin{pmatrix} dp \\ dq \end{pmatrix}=\begin{bmatrix} K^* & J^* \\ J^* & 3G^* \end{bmatrix}\begin{pmatrix} d\varepsilon_v \\ d\varepsilon_s \end{pmatrix} \tag{4}$$

where we use the asterisk sign in K^*, G^*, and J^* to emphasize the fact that with the presence of J^* the material is no longer isotropic, so that K^* and G^* are not conventional bulk and shear moduli anymore. J^* is a parameter expressing the cross dependence of the shear behavior on the volumetric behavior and vice versa.

An alternative is to use an elastic constitutive equation in terms of a compliance matrix (Atkinson and Richardson 1985; Lings et al. 2000)

$$\begin{pmatrix} d\varepsilon_v \\ d\varepsilon_s \end{pmatrix}=\begin{bmatrix} 1/K' & 1/J' \\ 1/J' & 1/3G' \end{bmatrix}\begin{pmatrix} dp \\ dq \end{pmatrix} \tag{5}$$

where in this case we used the apostrophe sign for the elastic moduli to distinguish them from the modulus presented in Eq. (4). No equivalence between the K', G' and K^*, G^* parameters exists unless for isotropic conditions ($J'=\pm\infty$ and $J^*=0$). Conversion between the two sets of parameters can be taken by inverting the matrices.

In this paper, we will first use the triaxial form of the potential functions as suggested in Eq. (3), so that the constitutive relation will have the same structure as in Eq. (5). We will later expand them by replacing the triaxial variables in the potential functions through Eqs. (1) and (2) so that we could use them for solution of two-dimensional (2D) and 3D BVP's.

Versatile Potential Function

Consider Gibbs free energy function of the form

$$g_e[p,q] = -\frac{p^{2-m} - (2-m)p \cdot p_0^{1-m}}{\overline{K}(2-m)(1-m)p_r^{1-m}} - \frac{q^2}{6\overline{G}p_r^{1-n}p^n} + \frac{q_0(2qp_0 - nq_0p)}{6\overline{G}p_r^{1-n}p_0^{1+n}} \tag{6}$$

where n, m, $\overline{K}$, and $\overline{G}$=material constants and p_r=reference pressure (conveniently taken as 1 kPa). The complete expressions for the strains are given by the properties of the Legendre transformation in Eq. (3)

$$\varepsilon_v = -\frac{\partial g_e}{\partial p} = \frac{p^{1-m} - p_0^{1-m}}{\overline{K}(1-m)p_r^{1-m}} - \frac{nq^2}{6\overline{G}p_r^{1-n}p^{1+n}} + \frac{nq_0^2}{6\overline{G}p_r^{1-n}p_0^{1+n}} \tag{7}$$

$$\varepsilon_s = -\frac{\partial g_e}{\partial q} = \frac{q}{3\overline{G}p_r^{1-n}p^n} - \frac{q_0}{3\overline{G}p_r^{1-n}p_0^n} \tag{8}$$

Note that both of these expressions give zero elastic strains for initial conditions $p=p_0$ and $q=q_0$. In the following, we are going to explore some properties of the proposed hyperelastic constitutive relationship.

Stiffness and Compliance Matrices

Differentiating by the stresses produces the elastic compliance matrix

$$C = \begin{bmatrix} \frac{-\partial^2 g_e}{\partial p^2} & \frac{-\partial^2 g_e}{\partial p \partial q} \\ \frac{-\partial^2 g_e}{\partial q \partial p} & \frac{-\partial^2 g_e}{\partial q^2} \end{bmatrix} = \begin{bmatrix} \frac{1}{\overline{K}p_r(p/p_r)^m} + \frac{\overline{n}\eta^2}{3\overline{G}p_r(p/p_r)^n} & -\frac{n\eta}{3\overline{G}p_r(p/p_r)^n} \\ -\frac{n\eta}{3\overline{G}p_r(p/p_r)^n} & \frac{1}{3\overline{G}p_r(p/p_r)^n} \end{bmatrix} \tag{9}$$

where $\eta = q/p$=stress ratio and $\overline{n} = n(n+1)/2$. The product of $n\eta$ can be identified as a measure of anisotropy, since when it is equal to zero the material becomes isotropic. The fact that the off-diagonal terms depend on the stresses and reduce to zero on the isotropic axis ($\eta=0$) represents what is commonly termed ''stress induced cross-anisotropy.'' In order to account for the ''inherent cross-anisotropy'' of the material it is possible to add another term to the potential function (6), for example the term $(q-q_0)(p-p_0)/J_0$ that will add $-1/J_0$ to the off-diagonal terms in Eq. (9), so that J_0 could be interpreted as the inherent cross-coupling parameter. This paper, however, is concerned only with stress induced anisotropic materials, which can be described by an infinite $|J_0|$.

When $n=0$ the shear modulus is pressure independent, the coupling off-diagonal terms and the induced dilatancy term in the bulk modulus due to shear modulus dependency on pressure are vanished, so that the model reduces to an isotropic model. If we use $n=m=0$, the model further degenerates to an isotropic linear elastic model. The important observation here is that when the elastic behavior is properly derived from a potential function, any attempt to introduce a shear modulus, which is pressure dependent, also introduces coupling terms and an additional dilatancy term due to shear modulus. Therefore, all isotropic models where the shear modulus and bulk modulus are both pressure dependent, simply do not conserve energy (Zytynski et al. 1978).

The elastic stiffness matrix for this model is derived by inversion of the compliance matrix:

$$D = \frac{3\overline{G}}{3\overline{G} - \eta^2 \underline{n}\overline{K}(p/p_r)^{m-n}} \times \begin{bmatrix} \overline{K}p_r(p/p_r)^m & n\eta\overline{K}p_r(p/p_r)^m \\ n\eta\overline{K}p_r(p/p_r)^m & 3\overline{G}p_r(p/p_r)^n + \eta^2\overline{n}\overline{K}p_r(p/p_r)^m \end{bmatrix} \tag{10}$$

where $\underline{n} = n(n-1)/2$. Before we investigate the form of the shear and bulk moduli it is important to note that their precise definition is sometimes ambiguous.

Apparent Shear Modulus

We use the term ''apparent'' in order to emphasize that this is the direct measurable shear modulus, which can be extracted when no coupling exists (i.e., on isotropic axis). In this case the shear modulus is dependent on the pressure and is given by Eqs. (4), (5), and (9) and the condition that η equals zero as

$$G^*(p,q)|_{(\eta=0)} = G'(p,q)|_{(\eta=0)} = \overline{G}p_r(p/p_r)^n \tag{11}$$

This kind of dependency of shear modulus on the mean normal stress was observed by many writers (Hardin 1978; Houlsby and Wroth 1991; Jovicic and Coop 1997; Rampello et al. 1997; Atkinson 2000). For example, Rampello et al. (1997) used the following expression for clays:

$$G(p,p_y) = S^* p_r(p/p_r)^{n_1}(p_y/p)^{n_2} \tag{12}$$

where S^*, n_1, and n_2=material constants and p_y=preconsolidation pressure. It can be seen that for normally consolidated clays ($p=\underline{p_y}$) the expression in Eq. (12) is the same as in Eq. (11) by using $G=S^*$ and $n=n_1$. It can be argued that the model proposed here lacks the preconsolidation dependency for overconsolidated clays. Nevertheless, the elastic shear modulus in Eq. (11) is found to be a good compromise between accuracy, thermodynamic consistency and ease of implementation. It is also found to be the most general: It can produce constant modulus ($n=0$); linear pressure dependent modulus ($n=1$); or power function of pressure dependent modulus, typically determined from small strains measurements to be around $n \cong 0.65$ for clays (Rampello et al. 1997) and $n \cong 0.5-0.7$ for sands (Jovicic and Coop 1997).

Apparent Bulk Modulus

The apparent bulk modulus determined from the potential function has the same form as the apparent shear modulus (11), but with different power constant m

$$K^*(p,q)|_{(\eta=0)} = K'(p,q)|_{(\eta=0)} = \overline{K}p_r(p/p_r)^m \tag{13}$$

For materials such as metals, the elastic bulk modulus is usually taken as pressure independent, which can be achieved by using $m=0$, while soils are regarded to have a strong dependency on the mean effective stress. For example, sands are sometimes con-

sidered to have $m \cong 0.5$. Critical-state models most commonly consider the elastic bulk modulus to be a linear function of p $(m=1)$. Unfortunately, this leads to a singularity in the proposed formulation, because the first terms of the Gibbs free energy potential (6) and of the volumetric strain (7) are divided by $(1-m)$. Though using m approaching to 1 (say $m=0.999...$) will practically yield the same stress-strain curve, this might cause numerical problems, therefore it is preferable to search for another solution to this case.

By taking a limit of Eq. (9) for m approaching unity, the first term of the potential function acquires a new form

$$\lim_{m\to 1}\left(-\frac{p^{2-m}-(2-m)p\cdot p_0^{1-m}}{\bar{K}(2-m)(1-m)p_r^{1-m}}\right) = -\frac{p}{K}\left(\mathrm{Ln}\left[\frac{p}{p_0}\right]-1\right) = -\kappa^* p\left(\mathrm{Ln}\left[\frac{p}{p_0}\right]-1\right) \tag{14}$$

where $1/\bar{K}$ is replaced by κ^*, which is the elastic compressibility index that produces straight swelling lines in $\varepsilon_v - \ln(p)$ space (see Butterfield 1979; Hashiguchi 1995). The complete form of the Gibbs potential function for the case of $m=1$ is given by

$$\bar{g}_e[p,q] = -\kappa^* p\left(\mathrm{Ln}\left[\frac{p}{p_0}\right]-1\right) - \frac{q^2}{6\bar{G}p_r^{1-n}p^n} + \frac{q_0(2q-q_0 pn)}{6\bar{G}p_r^{1-n}p_0^n} \tag{15}$$

where we use the bar notation to distinguish between this form and the general form in Eq. (6). As might be expected, differentiation of the first part of $\bar{g}_e[p,q]$ by p produces expression equal to the limit of the first term of the volumetric strain in Eq. (7) for m approaching unity

$$\lim_{m\to 1}\left(\frac{p^{1-m}-p_0^{1-m}}{\bar{K}(1-m)p_r^{1-m}}\right) = \frac{1}{K}\mathrm{Ln}\left[\frac{p}{p_0}\right]\left\{ = \frac{\partial\left(\kappa^* p\,\mathrm{Ln}\left[\frac{p}{p_0}\right]\right)}{\partial p} = \kappa^*\mathrm{Ln}\left[\frac{p}{p_0}\right]\right\} \tag{16}$$

and so the full expression of the volumetric strain is given by

$$\varepsilon_v = -\frac{\partial \bar{g}_e}{\partial p} = \kappa^*\mathrm{Ln}\left[\frac{p}{p_0}\right] - \frac{nq^2}{6\bar{G}p_r^{1-n}p^{1+n}} + \frac{nq_0^2}{6\bar{G}p_r^{1-n}p_0^{1+n}} \tag{17}$$

The shear strain derived from $\bar{g}_e[p,q]$ is the same as given by Eq. (7). Differentiating the strains (8) and (17) by the stresses yields the elastic compliance matrix

$$C = \begin{bmatrix} \frac{\kappa^*}{p} + \frac{\bar{n}\eta^2}{3\bar{G}p_r(p/p_r)^n} & -\frac{\eta n}{3\bar{G}p_r(p/p_r)^n} \\ -\frac{\eta n}{3\bar{G}p_r(p/p_r)^n} & \frac{1}{3\bar{G}p_r(p/p_r)^n} \end{bmatrix} \tag{18}$$

and by inversion of the compliance matrix we obtain the elastic stiffness matrix

$$D = C^{-1} = \frac{3\bar{G}\kappa^*}{3\bar{G}\kappa^* - \eta^2\underline{n}(p/p_r)^{1-n}}\begin{bmatrix} \frac{p}{\kappa^*} & \frac{p}{\kappa^*}n\eta \\ \frac{p}{\kappa^*}n\eta & 3\bar{G}p_r(p/p_r)^n + \eta^2\bar{n}\frac{p}{\kappa^*} \end{bmatrix} \tag{19}$$

Relation to Existing Stored Energy Functions

Particular Cases

Assume the second version of the Gibbs function (15) for the case $n=0$ and $q_0=0$ such that the volumetric and shear strain takes the following form:

$$\varepsilon_v = \kappa^*\mathrm{Ln}\left[\frac{p}{p_0}\right]; \quad \varepsilon_s = \frac{q}{3\bar{G}p_r} \tag{20}$$

then it is possible to extract the mean effective and deviator stress as

$$p = p_0\exp\left(\frac{\varepsilon_v}{\kappa^*}\right); \quad q = 3G\varepsilon_s \tag{21}$$

where we replace the product of $\bar{G}p_r$ by the conventional shear modulus of G since the nondimensional format is not necessary for $n=0$. After some elaboration, by using Eqs. (3), (15), and (21) we can obtain the expression for the Helmholtz free energy potential function

$$\bar{f}_e[\varepsilon_v,\varepsilon_s] = p_0\kappa^*\exp(\varepsilon_v/\kappa^*) + \frac{3G\varepsilon_s^2}{2} \tag{22}$$

This potential function was originally proposed by Houlsby (1985). Because critical-state models often use both bulk modulus and shear modulus proportional to pressure, Houlsby (1985) suggested to modify the potential to

$$\bar{f}_e[\varepsilon_v,\varepsilon_s] = p_0\kappa^*\exp(\varepsilon_v/\kappa^*) + \frac{3}{2}\alpha p_0\exp(\varepsilon_v/\kappa^*)\varepsilon_s^2 \tag{23}$$

in which the shear modulus G has simply been replaced by $\alpha p_0\exp(\varepsilon_v/\kappa^*)$. The presence of the extra term in ε_v results in more complicated expression for p on differentiation

$$p = p_0\exp\left(\frac{\varepsilon_v}{\kappa^*}\right)\beta; \quad q = 3\alpha p_0\exp\left(\frac{\varepsilon_v}{\kappa^*}\right)\varepsilon_s \tag{24}$$

where

$$\beta = 1 + 3\alpha\varepsilon_s^2/2\kappa^* \tag{25}$$

Another differentiation by the strains leads to the modulus matrix in two optional forms

$$D = p_0\exp\left(\frac{\varepsilon_v}{\kappa^*}\right)\begin{bmatrix} \frac{\beta}{\kappa^*} & \frac{3\alpha\varepsilon_s}{\kappa^*} \\ \frac{3\alpha\varepsilon_s}{\kappa^*} & 3\alpha \end{bmatrix} = \begin{bmatrix} \frac{p}{\kappa^*} & \frac{p}{\kappa^*}\eta \\ \frac{p}{\kappa^*}\eta & 3\frac{p}{\beta}\alpha \end{bmatrix} \tag{26}$$

The presence of the off-diagonal terms in the second option in Eq. (26) indicates that the elastic shear and volumetric responses are coupled for a general loading path, and that the coupling magnitude is proportional to the stress ratio η. A very similar (though not identical) stiffness matrix (19) can be obtained by utilizing the

potential in Eq. (15) with $n=1$. Note also the presence of β (25) within the bulk modulus in the first Eq. (26), which indicates the same effects of additional dilatancy term due to shear modulus variation with presure.

Boyce (1980) suggested on the basis of reciprocity of strains $(\partial\varepsilon_v/\partial q=\partial\varepsilon_s/\partial p)$, a compliance moduli matrix which takes the following form:

$$C=\begin{bmatrix} \dfrac{\partial\varepsilon_v}{\partial p} & \dfrac{\partial\varepsilon_v}{\partial q} \\ \dfrac{\partial\varepsilon_s}{\partial p} & \dfrac{\partial\varepsilon_s}{\partial q} \end{bmatrix}=\begin{bmatrix} \dfrac{1-n}{\bar{K}p^n}+\dfrac{\bar{n}\eta^2}{3\bar{G}p^n} & -\dfrac{n\eta}{3\bar{G}p^n} \\ -\dfrac{n\eta}{3\bar{G}p^n} & \dfrac{1}{3\bar{G}p^n} \end{bmatrix} \tag{27}$$

Although Boyce (1980) did not present the energy potential function for his model, the apparent tangential shear and coupling modulus correspond to those in Eq. (9) for $m=n$ and $p_r=1$. However, the tangential bulk modulus is different: the term $(1-n)/\bar{K}p^n$ comes instead of $1/\bar{K}p^n$. This seemingly minor difference causes Boyce's (1980) model to yield apparent bulk modulus $K^*(p,q)|_{(\eta=0)}=\bar{K}p^n/(1-n)\underset{n=1}{\rightarrow}\infty$ that approaches infinity, for linear pressure-dependent bulk modulus (i.e., $n=1$), which is often used in cam-clay plasticity. Altogether, we should also remind the important feature, which the proposed potential function (6) allows by differing between the power dependency of shear and bulk moduli (using $n\neq m$).

Undrained Triaxial Loading

Houlsby (1985) showed that the undrained stress paths (identical to contours of constant ε_v) obtained from the potential function in Eq. (23), are given by the parabola

$$q=\sqrt{6\alpha\kappa^* p_1(p-p_1)} \tag{28}$$

where p_1=intercept of the parabola on the p axis.

It can be shown that the undrained stress paths derived from the elastic stiffness matrix (10) for the special case of $m=n$ are given by

$$q=\sqrt{\frac{6\bar{G}}{\bar{K}}p^2\left(\frac{p^{n-1}-p_1^{n-1}}{n(n-1)}\right)} \tag{29}$$

and for $m=n=1$ [either according to the elastic stiffness matrix in Eq. (19) or by taking a limit operation on Eq. (29)] are given by

$$q=\sqrt{6\bar{G}\kappa^* p^2\mathrm{Ln}(p/p_1)} \tag{30}$$

The contours of the undrained stress paths for Houlsby's potential (23) and for the proposed potential for typical values of parameters ($m=n=0.65$) are, respectively, illustrated in Figs. 1(a and b), together with modified cam-clay yield locus. Also shown in Fig. 1 (in dashed lines) are lines that represent the maximum attainable stress ratio for $p\rightarrow\infty$. For Houlsby's potential (see Borja et al. 1997), a maximum attainable stress ratio is $\sqrt{3\alpha\kappa^*/2}$. In that model [Eqs. (23) and (26)], $\mathrm{Det}(D)=0$ yields the same value of stress ratio, so singularity cannot occur since $(q/p)_{\max}=(q/p)_{\text{singular}}$. In the proposed versatile function [Eqs. (6) and (10)] a maximum attainable stress ratio $(q/p)_{\max}$ is given by $\sqrt{3\bar{G}/n\bar{K}}$, while $\mathrm{Det}(D)=0$ in case $m=n$ yields the slope $\sqrt{3\bar{G}/n^2\bar{K}}$. In this case, no singularity will be encountered as long as $n\leqslant 1$.

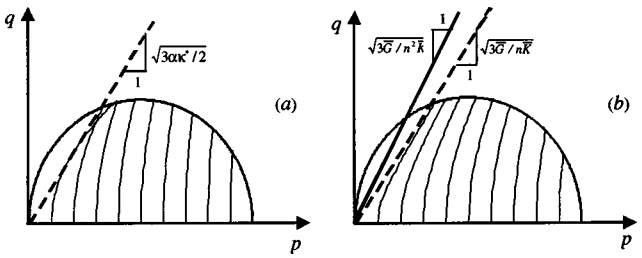

Fig. 1. Undrained stress paths for elastic behavior inside yield locus: (a) Houlsby (1985) and (b) new function (for $n=m=0.65$)

Hyperplastic Model

Hyperplasticity

Hyperplasticity is an approach to plasticity based on thermomechanical principles as suggested by Ziegler (1977, 1983) and described by Houlsby (1981), Collins and Houlsby (1997), and Houlsby and Puzrin (2000), and which is also closely related to the works of Halphen and Nguyen (1975), Martin and Nappi (1990), and Maugin (1992). An advantage of this approach is that it can describe a rather broad class of models which are automatically guaranteed to obey the First and Second Laws of Thermodynamics. By analogy with elasticity theory where hyperelastic behavior is derived from a single scalar potential function, the hyperplastic behavior is derived from two potentials, conveniently taken as either the Gibbs or Helmholtz free energy and the dissipation function.

This paper utilizes hyperplasticity, rather than supplies its theoretical details; for details, readers can refer to the above references and to the thesis work by Einav (2002).

Automatic Derivation of Incremental Response

Normally, a new constitutive model would require a new procedure for derivation of the incremental response. For models generated within the framework of hyperplasticity, this derivation has been unified and is performed semi-automatically by a computer routine using the built-in programming language *FISH*, specially embedded in the commercially available FD code, *FLAC ver 3.4* (Itasca 2000). An advantage of the hyperplastic approach is in the compactness of its formulation: Two scalar potential functions define a model completely. By that, the whole process of constitutive modeling has been considerably simplified. By modifying these functions, new models can be easily developed, and a complete derivation of the incremental relations for a constitutive model is then automatically produced. The entire constitutive response can be obtained for each zone in the FD grid and the corresponding solutions for BVP's can be obtained.

Due to a lack of space we do not intend to elaborate on how the incremental response of a specific model can be derived. Instead, the reader is referred to the work of Einav (2002), which presents the code in details.

Hyperplastic Model

In the following we will formulate a hyperplastic modified cam-clay (MCC) model with an incorporated hyperelastic component defined by the Gibbs free energy function $\bar{g}_e[p,q]$ [Eq. (15)]. Two energy functions define the proposed hyperplastic model; these are the specific Gibbs free energy function

$$g[p,q,\alpha_v,\alpha_s]=\overline{g}_e[p,q]-(p\alpha_v+q\alpha_s)+\frac{p_c(\alpha_v)}{2}(\lambda^*-\kappa^*) \tag{31}$$

and dissipation function

$$d^g[\alpha_v,\alpha_s]=\frac{p_c(\alpha_v)}{2}\sqrt{\dot{\alpha}_v^2+M^2\dot{\alpha}_s^2}\geq 0 \tag{32}$$

where, in this particular model, the internal variables α_v and α_s correspond to the volumetric and shear plastic strains respectively; $p_c(\alpha_v)=p_{co}\exp(\alpha_v/(\lambda^*-\kappa^*))$=intercept of the yield surface on the p axis; M=coefficient of friction ($q=Mp$ is the failure criterion); p_{co}=initial intercept of the yield surface on the p axis; and λ^*=compressibility soil index for virgin loading. Using a degenerate Legendre transformation on the dissipation (32), and since $-\partial g/\partial\alpha_v=p-p_c(\alpha_v)/2$ and $-\partial g/\partial\alpha_s=q$, it can be easily shown that the yield function in the Cauchy stress space takes the following form:

$$y^g(p,q,\alpha_v)=[p-p_c(\alpha_v)/2]^2+(q/M)^2-[p_c(\alpha_v)/2]^2=0 \tag{33}$$

which corresponds to the conventional MCC yield surface. Isotropic hardening is introduced using function (32) such that it will result in the elliptical yield surface changing its size with plastic strains but always passing through the origin.

Functions (31) and (33) were used as an input for the computer routine implemented in *FLAC*, which automatically defined the incremental response for the model. Within the yield surface the behavior is hyperelastic defined by the compliance matrix (18). When the plastic loading takes place, this compliance matrix defines elastic strain increment, while the plastic strain increment is the same as in the conventional MCC model with associated flow rule.

Conventional Hypoelastic-Plastic Model

At this stage we have a complete model, which is consistent with thermodynamic principles both in elastic and plastic modes of behavior. Let us now imagine that we are not concerned with thermodynamics, but we would like to develop a conventional elastoplastic model with the same basic components and parameters as the hyperplastic model developed in the previous section. What kind of model would we end up with?

Assuming decomposition of incremental strain tensor into the elastic and plastic components, a conventional elastoplastic constitutive relation could be written as

$$\begin{pmatrix} d\varepsilon_v \\ d\varepsilon_s \end{pmatrix}=\begin{bmatrix} \dfrac{\kappa^*}{p} & 0 \\ 0 & \dfrac{1}{3\overline{G}p_r(p/p_r)^n} \end{bmatrix}\begin{pmatrix} dp \\ dq \end{pmatrix}+\begin{pmatrix} d\varepsilon_v^p \\ d\varepsilon_s^p \end{pmatrix} \tag{34}$$

The first term in the right side is the incremental elastic strain vector. Its compliance matrix reflects pressure dependency of the bulk and shear moduli and therefore it is a hypoelastic material. This dependency is identical to the proposed hyperelastic compliance matrix (18) with two "minor" differences: The off-diagonal coupling terms and the additional dilatancy term due to shear modulus dependency on pressure are vanishes. This is not surprising, because, as we remember, these terms are needed to ensure that the model conserves energy, which is not of our concern here.

The plastic strains are computed by invoking an associate flow rule $\left(\begin{smallmatrix} d\varepsilon_v^p \\ d\varepsilon_s \end{smallmatrix}\right)=\lambda\left(\begin{smallmatrix} \partial F/\partial p \\ \partial F/\partial q \end{smallmatrix}\right)$ in the usual way, where the yield function F is the same function as in Eq. (33). To complete the isotropic hypoelastic-based elastoplastic model definition we determine the plastic multiplier λ by imposing the plastic consistency condition of $dF(p,q,\varepsilon_v^p)=0$. Thus, the plastic strain increment is again the same as in the conventional MCC model with associated flow rule.

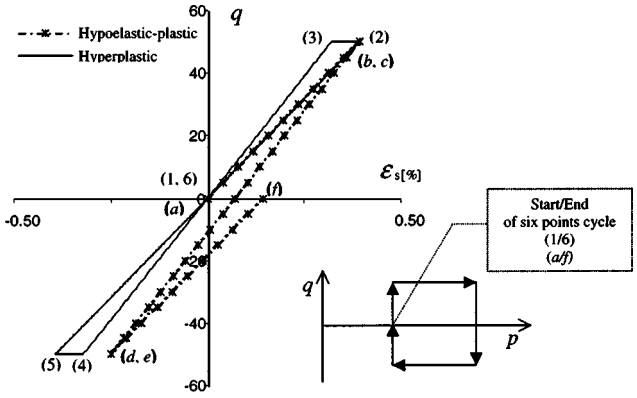

Fig. 2. Stress-strain curves for closed-loop stress path [hypoelastic-plastic model numerated by $(a,b\ldots)$ and hyperplastic model numerated by (1,2...)]

At this stage we have two elastoplastic models. One is a straightforward MCC-based elastoplastic model with a hypoelastic relationship for elastic component. Our guess is that a vast majority of geotechnical engineers will be completely content with its theoretical soundness even being aware of the fact that it might violate the First Law of Thermodynamics. Another model is almost identical but with a hyperelastic relationship for elastic component, which allows for the First Law of Thermodynamics to be satisfied. In fact, being utilized within the hyperplastic framework this model guarantees that the Second Law is satisfied too, but this is of a minor importance in this study. What is of major importance, it is to try and assess whether violation of the energy conservation law has any practical significance for solution of geotechnical BVPs.

Behavior of the Models in a Closed-Loop Stress Cycle

Zytynsky et al. (1978) have demonstrated that in the version of MCC models, where the Poisson's ratio is constant and the bulk and shear modulus are both linear dependent on pressure, energy could be extracted in a closed loading cycle. The hyperelastic component of the hyperplastic model presented in this paper allows for this fallacy to be avoided. In order to illustrate this fact we performed a closed-loop stress cycle (Fig. 2) for both the hyperplastic and the hypoelastic-plastic models. Because we are studying the elastic component, the chosen path is performed entirely within the yield surface.

The deviatoric stress-strain curve for this stress path is presented in Fig. 2. In order to be consistent with Zytynsky et al. (1978) the parameters m and n were taken as unity and the rest of the parameters have values typical for MCC parameters. A thermomechanical requirement is that if no yielding occurs, residual strain at the end of the cycle $\Delta\varepsilon_{ij}^e=0$. In fact, at that point the residual deviatoric strain for the hyperplastic model indeed equals to zero, in contrast to the hypoelastic-plastic model where it accumulates as the cycle proceeds. Apart from the thermomechani-

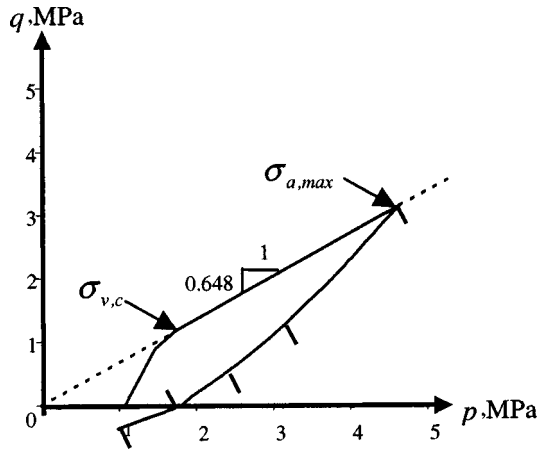

Fig. 3. Stress path prior to undrained shearing (Borja et al. 1997)

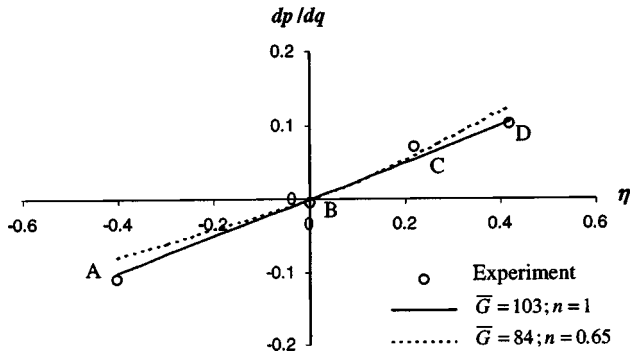

Fig. 4. Variation of dp/dq with stress ratio $\eta = q/p$

cal fallacy this leads to the rather annoying fact that a sequence of infinitesimal stress cycles may lead to accumulation of a final strain.

It should be noted that when the mean effective stress is kept constant, the deviator stress-strain curves are parallel. When constant deviatoric stress is applied, the hypoelastic-plastic model does not experience shear strains, due to the choice of isotropic elastic stiffness matrix. The hyperplastic model, however, undergoes shear straining due to the coupling, which eventually enables the deviatoric stress-strain curve to return back to zero strain at the end of the cycle.

Evaluation of the Models' Prediction of Laboratory Test Data

The predictive capability of the hyperplastic model is validated herein. Since the major difference between the hypoelastic-plastic model and the hyperplastic model concerns to the elastic component of the formulation, we examine them against test data within the yield surface. Borja et al. (1997) described the testing program and experimental results for stiff overconsolidated Vallericca clay in order to validate their own hyperelastic-plastic model, which was constructed using Houlsby's (1985) potential function. The special stress-path prior to the undrained shearing phase was designed to assure that at least during initial stages of shearing the clay behaved according to its elastic properties. This set of data has also been found appropriate for evaluation of the models described in this paper.

Description of the Undrained Triaxial Testing Program by Borja et al. (1997)

Prior to triaxial testing, oedometer tests indicated that the block samples had been subjected to an in situ maximum vertical effective stress of about $\sigma_{v,c} \approx 2.6$ MPa. Triaxial tests, which were carried out on five effectively identical samples, started by anisotropic consolidation to an effective axial stress of $\sigma_{a,\max} = 6.75$ MPa that is about 2.6 times $\sigma_{v,c}$ along a path corresponding to a constant stress ratio of $q/p = 0.684$ (or an equivalent lateral pressure coefficient that was estimated as $K_0 = 0.53$). Four of the five specimens were next unloaded to overconsolidation ratios of 1.7, 2.4, 3.8, and 8.9 corresponding to Points D, C, B, and A, respectively, along the path shown in Fig. 3 (here, OCR $= \sigma_{a,\max}/\sigma_{a,0}$, where $\sigma_{a,0}$ is the final value of the effective axial stress on unloading prior to undrained shearing). Next, undrained compressive shear tests were carried out.

Calibration of the Model Parameters

The calibration of the model parameters is initialized by using the elastic compressibility parameter $\kappa^* = 0.013$, that was obtained by Borja et al. (1997) from a plot of consolidation curves for four triaxial samples on v-$\log p$ (where $v = 1 + e$ is the specific volume). From the same graph, it can be concluded that the compressibility soil index for virgin loading $\lambda^* = 0.117$. Though this parameter is of no interest for this section of the paper, because it relates to the plastic behavior of the models, we shall need it later for solutions of BVPs.

The calibration of parameters $\overline{G}$ and n for both the hypoelastic-plastic and the hyperplastic models was performed using procedure proposed by Borja et al. (1997). Fig. 4 presents the measured values of dp/dq plotted versus the stress ratio $\eta = q/p$ at the beginning of the undrained stress paths. Note that the measured value of the initial slope dp/dq is zero only in the vicinity of the stress ratio $\eta \cong 0$ (Test B). It is also noted that when η is negative the slope dp/dq is negative (as in Test A), and when η is positive the slope dp/dq is positive (see Tests C and D). This behavior indicates that the material does indeed exhibit pressure-induced cross anisotropy due to volumetric-deviatoric coupling, a trend that is captured by the hyperplastic model. A hypoelastic-plastic model which utilizes pressure dependent shear modulus but neglects the coupling terms, cannot possibly capture this behavior, because dp/dq will always be zero for any stress ratio.

According to Eq. (19), the slope dp/dq for an undrained stress-path ($d\varepsilon_v = 0$) can be written as

$$\frac{dp}{dq} = \frac{np\eta}{3\overline{G}\kappa^* p_r (p/p_r)^n + \overline{n}p\eta^2} \tag{35}$$

which in case of $n = 1$ reduces to

$$\frac{dp}{dq} = \frac{\eta}{3\overline{G}\kappa^* + \eta^2} \tag{36}$$

Using the least-square deviation procedure for the case of $n = 1$, we obtain $\overline{G} = 103$ which fits the data with great accuracy (the straight solid line in Fig. 4, which is nearly linear).

Parameters $\overline{G}$ and n are determined here to fit phenomenon caused by stress-induced cross-anisotropy. Clearly, a more natural way would be to determine these parameters experimentally from the seismic lab tests or from the static tests with local deformation

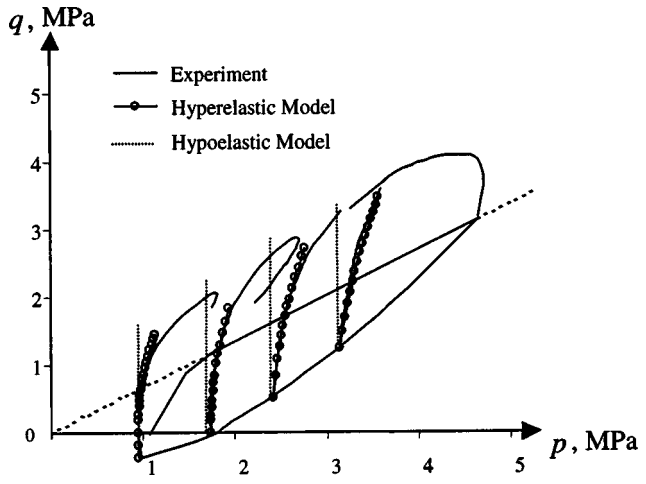

Fig. 5. Model's prediction of undrained triaxial test

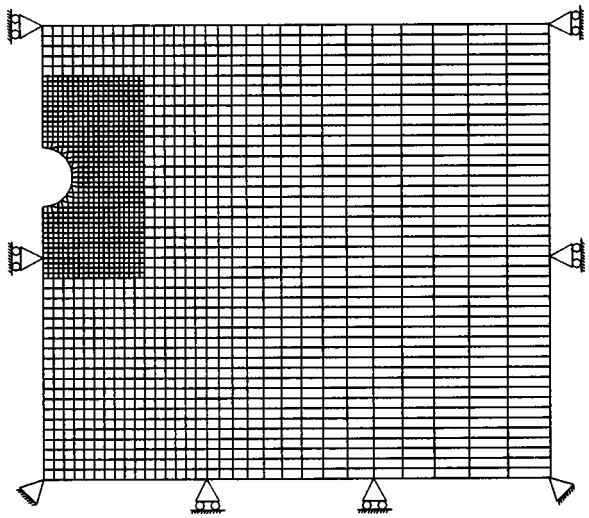

Fig. 6. Typical finite-element mesh

measurements. Unfortunately this kind of data is not available to the writers. However, existing experimental evidence for overconsolidated clays suggests that $n=0.65$ would be a reasonable assumption, covering a wide range of clays (e.g., Rampello et al. 1997; Stallebrass and Taylor 1997). Unfortunately, it is impossible to make a similar assumption with respect to G, because this parameter varies significantly for different clays. Therefore, it had to be also determined by fitting Eq. (35) to the data in Fig. 4. The value of $\bar{G}=84$ provided the best fit, which is presented by the dashed line in Fig. 4. As is seen this line also fits the data reasonably well. In the following we shall carry on with the both sets of parameters to investigate sensitivity of the BVP solutions to variation in these parameters.

Comparison of the Predictions

Fig. 5 shows a comparison between the measured undrained stress paths and predicted ones (within the yield surface) by both hypoelastic-plastic and the hyperplastic models with $\bar{G}=103$ and $n=1$. The predictions provided by these models for the second set of parameters $\bar{G}=84$ and $n=0.65$ are practically identical (respectively) to those in Fig. 5. This is hardly surprising, considering the way these parameters were calibrated in the previous section. The hypoelastic-plastic model fails completely in capturing the curvature of the undrained stress paths within the yield surface. The hyperplastic model, on the contrary, provides good prediction for undrained stress paths for heavily overconsolidated clays. We do not intend to claim the same for the case of lightly overconsolidated clays (prediction for normally consolidated clay will be almost the same as using the MCC model). It seems that combining the new potential function within the framework of continuous hyperplasticity (Puzrin and Houlsby 2001a,b), could be used for lightly overconsolidated clays, since it can consider nonlinear plasticity within the large-scale yield surface.

Comparison of the Models' Prediction of Subsidence Induced by Tunnel Excavation

Zytynsky et al. (1978) suggested that energy conservation should have a significant effect when loading involves many stress reversals, while for monotonic loading it is solely of academic interest. However, there exists some evidence that for some monotonic loading conditions this effect can be significant as well. Lee and Rowe (1989) examined the influence of cross-anisotropic elastic parameters on results of linear elastic perfectly plastic finite element analysis of tunneling. In their study they modeled a soil, which had initial horizontal to vertical effective stress ratio $K_0<1$, and concluded that particular attention should be given to the ratio of independent shear modulus to vertical modulus. In the present and previous studies it has been shown that for the sake of energy conservation, elastic models that imply pressure-dependent shear modulus must incorporate cross-anisotropic modulus terms. Combining these two conclusions we may guess that for certain initial conditions of K_0, the induced anisotropy of the hyperplastic model could have some effect on solution of a BVP related to tunneling. This assumption will be explored in the following.

Description of the Boundary Value Problem

The BVP of surface subsidence induced by tunnel excavation has been solved for both the hyperplastic and the hypoelastic-plastic models. Even though that most often the problem requires 3D analysis, we are only interested in qualitative study, hence for simplicity we utilized the 2D plane strain assumption. The analysis is comprised from four sets of runs: each of the two models is utilized with two sets of parameters: ($\bar{G}=103$, $n=1$) and ($\bar{G}=84$, $n=0.65$). Each set of runs included seven runs of different ratios of tunnel crown depth to tunnel diameter (H/D), so that altogether 28 runs were carried out. Typical cross-section geometry is presented in Fig. 6. The two vertical boundaries permitted no horizontal displacement, and no vertical displacement was allowed along the bottom boundary. The water table is at the ground surface. The analysis was conducted using undrained conditions where pore pressure was allowed to develop but not dissipate because of the very law hydraulic conductivity of clay. Hydraulic boundary conditions allow for free development of pore pressure at the vertical and bottom boundaries. The unlined tunnel boundary is assumed to be impermeable, and change in pore pressure around the tunnel is assumed to occur only as a result of mechanical deformations. The top boundary enabled fluid to flow to and from the outside world by fixing the pore pressure to zero. Before the excavation process began, initial stress ratio K_0 was prescribed according to K_0

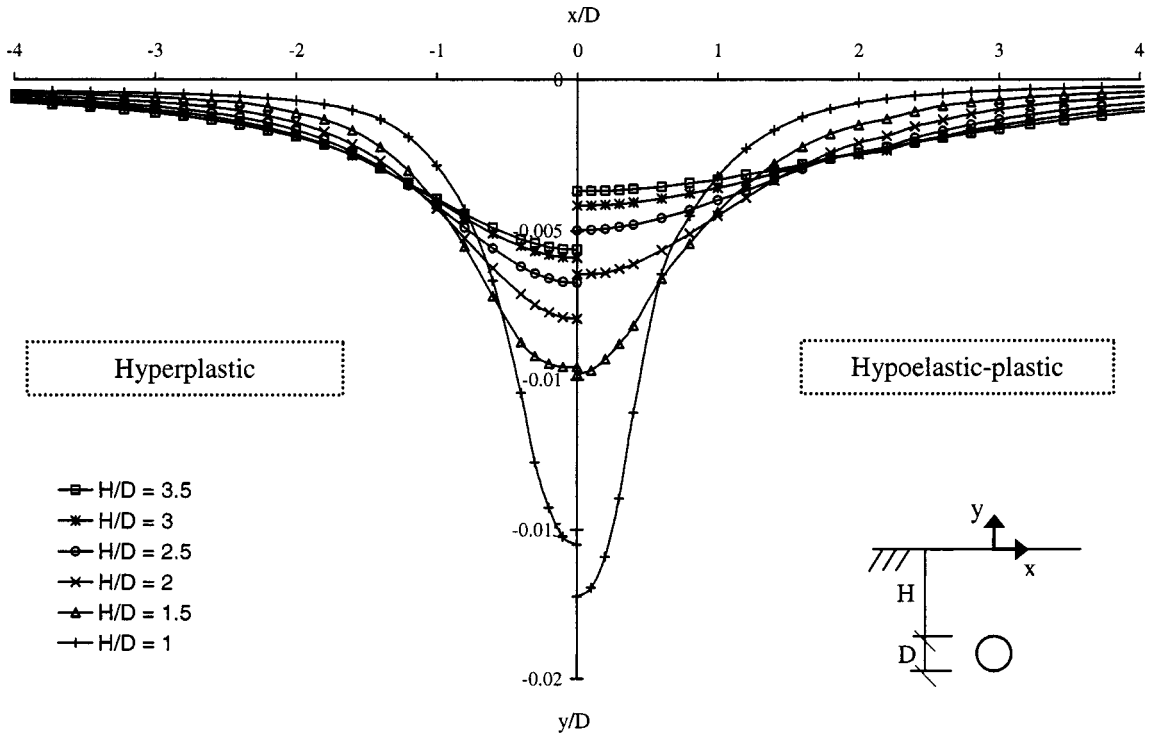

Fig. 7. Normalized settlement troughs at ground surface for different H/D ratios (for first set of parameters $\bar{G}=103$ and $n=1$)

$=(K_{0,\mathrm{NC}})\mathrm{OCR}^{\mathrm{Sin}\,\phi'}=(1-\mathrm{Sin}\,\phi')\mathrm{OCR}^{\mathrm{Sin}\,\phi'}$ in order to give characteristic site conditions. Since the model was validated only for OCRs within 1.7 to 8.9, we decided to perform the BVP calculations using OCR=2 thus we used $\underline{K}_0=0.71$ (for $\phi'=30°$) and $p_{c0}=\mathrm{OCR}\cdot p_0=2p_0$. As aforesaid, G and n were taken with correspondence to the particular set of runs, where for convenience we used $p_r=1$ MPa due to the high initial stress of 1 to 3.1 MPa. The rest of the model parameters were drawn from Borja et al. (1997): $\kappa^*=0.013$; $\lambda^*=0.15$; and $M=1.2$ (following from adopting $\phi'=30°$). After assigning the model parameters, equilibrium was achieved and then displacements were zeroed.

The excavation boundary conditions simulate removal of material from the tunnel region. First the finite element mesh inside the future tunnel perimeter was nullified and replaced by equivalent unbalanced forces. Next the unbalanced forces acting on the future tunnel lining were gradually decreased to simulate the removal of material from the finite-element mesh. Volume loss, which is defined as the volume of soil excavated in excess of the theoretical volume of excavation, was constantly monitored; this was calculated by measuring the volume of the surface settlement by assuming that for undrained conditions this volume equals the volume loss and thus the total volume remains constant. The calculation process was automatically cut off as soon as the volume lost reached the value of 3.3%. This value was taken from Addenbrooke et al. (1997) as a representative value at which the construction phase begun, and lining was installed.

Comparison of the Predictions

Fig. 7 presents the normalized settlement troughs at the ground surface for different H/D when using the first set of parameters ($\bar{G}=103$ and $n=1$). Generally as H/D grows, the ratio between settlements above the tunnel to those in the far field is decreasing for both models since the velocity field is more radiantly dispersed, but it decreases less for the hyperplastic model. Figs. 8(a and b) present the normalized maximum-settlement of the ground surface for the first and second set of parameters, respectively. Fig. 9 presents the relative difference between maximum settlements for hyperplastic and hypoelastic-plastic models: $\Delta=(y_{\max}^{\mathrm{HP}}-y_{\max}^{\mathrm{HEP}})/y_{\max}^{\mathrm{HEP}}\times 100\%$ (where the superscript "HP" stands for hyperplastic and "HEP" for hypoelastic-plastic model). For example, at $H/D=3.5$ the relative difference is $\Delta=54\%$ for $\bar{G}=103$ and $n=1$ and $\Delta=39\%$ for $\bar{G}=84$ and $n=0.65$. In general, there is an obvious difference between the models' prediction, tending to grow, as the tunnel is deeper. Note that the hypoelastic-plastic model is getting more nonconservative in the sense that it predicts shallower settlement troughs in case of deeper tunnels (when H/D is approximately more then $\sim$1.5 and $\sim$2.2 for the first and second set of runs, respectively), which are usually the practical cases.

For shallow tunnels, on the contrary, the hypoelastic-plastic model is more conservative, e.g., in $H/D=1.0$ the relative difference is $\Delta=-10\%$ for the first set of parameters and $\Delta=-23\%$ for the second one. The reason is probably implied in the fact that in these cases plastic flow region in the vicinity of the tunnel extends up to the soil surface and thus becomes the dominant phenomenon. In other words, the fact that there is a difference between the predictions is not based directly on the difference hypo- and hyperelasticity formulations, because for shallow tunnels, results are dominated by the plastic yielding. So, why is there still the difference, in spite of the fact that the plastic behavior described by the both models is basically the same?

The answer to this question is implied in Fig. 5: The undrained effective stress path predicted by the hyperelastic model deviates significantly from the vertical line predicted by the hypoelastic model. Because of that, these two paths hit the same yield surface far away from each other, leading to a significant difference in initial plastic yielding conditions. This conclusion is also true for

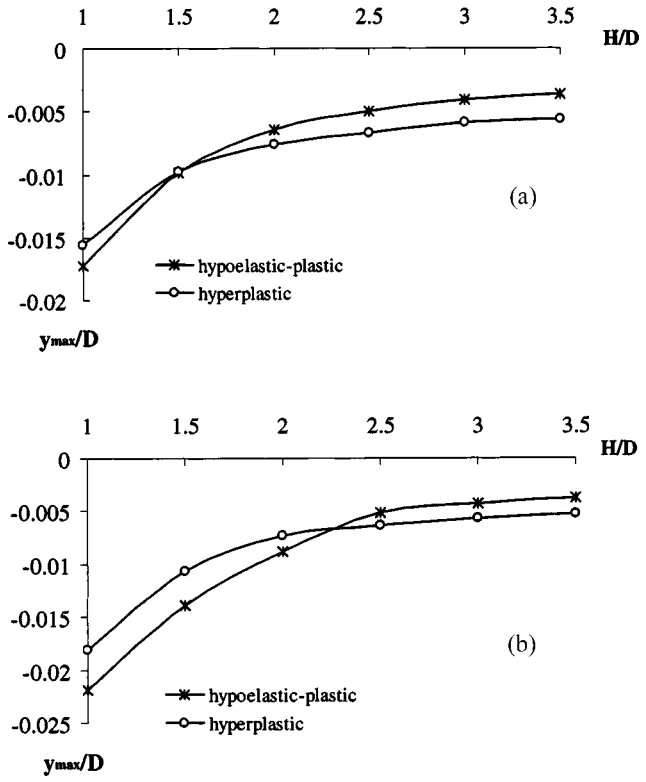

Fig. 8. (a) Normalized maximum-settlement of ground surface (for the first set of parameters $G=103$ and $n=1$) and (b) normalized maximum-settlement of ground surface (for the second set of parameters $G=84$ and $n=0.65$)

deeper tunnels, as illustrated in Fig. 10 presenting a close-up view of the yielding regions predicted by both models for the case of $H/D=3.5$ and volume loss of 3.3%. The differences between the shapes and dimensions of the corresponding regions are obvious. Clearly, the effect of this phenomenon on the ground surface settlements is more pronounced for shallow tunnels. Generally, in other BVPs where plastic yielding becomes more dominant, this phenomenon will probably be the main factor for difference between hypoelastic-plastic and hyperplastic models predictions.

Finally, it would be interesting to attempt to assess sensitivity of the hyperplastic model predictions to the choice of parameters. In Fig. 9 we also find the relative difference between maximum

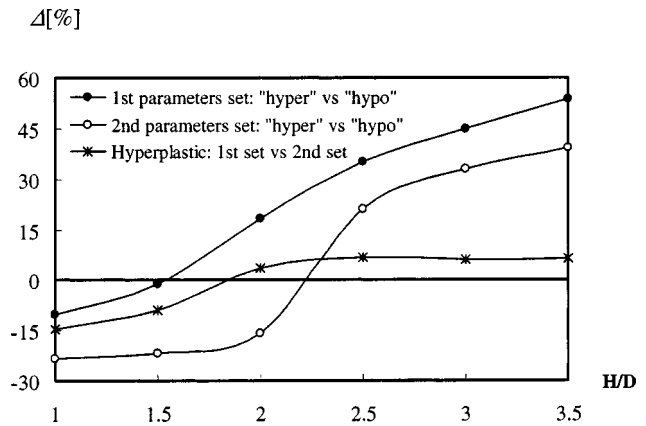

Fig. 9. Relative difference between models prediction

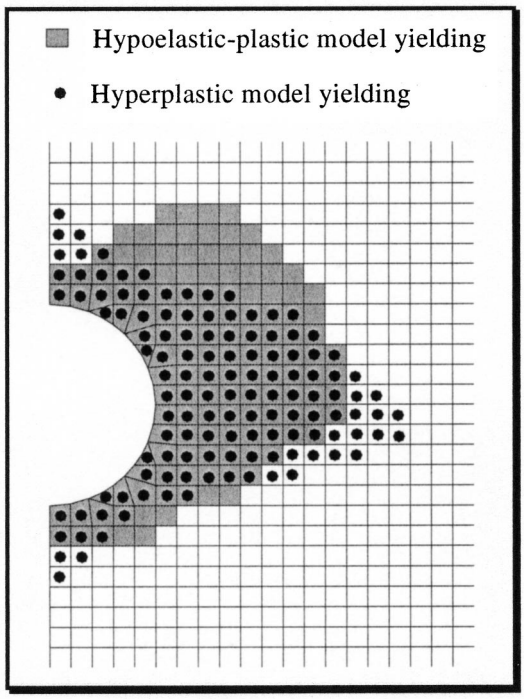

Fig. 10. Close-up view on yielding region for $H/D=3.5$ (for first set of parameters $G=103$ and $n=1$)

settlements as predicted by the hyperplastic model for the first ($G=103$ and $n=1$) and the second ($G=84$ and $n=0.65$) sets of parameters, plotted versus normalized tunnel depth. As is seen, the model predictions are not particularly sensitive to this significant variation in parameters, especially for deeper tunnels. When compared to the corresponding curves in Fig. 9 it can be concluded that even significant variation in the parameters of the hyperelastic model leads to smaller errors than those caused by the hypoelastic-plastic model using the same parameters, but neglecting energy conservation.

However, it would be wrong to generalize this conclusion to other BVPs, because of the particular way of calibration of these parameters (to provide the best fit to undrained effective stress paths within a region of high initial stresses of 1 to 3.1 MPa). More extensive parametric study is required to explore the sensitivity matter in depth.

Conclusions

The energy potential function presented herein is sufficiently versatile to cover a wide range of existing empirical relations for pressure dependent stiffness of soils. Utilization of these functions within hyperplastic constitutive framework allows for the resulting models to satisfy the Law of Energy Conservation for both elastic and plastic components of soil behavior. Apart from the theoretical rigor, a very important result of this approach is that it automatically implies stress-induced cross-anisotropy of the elastic component of soil behavior, which is also observed experimentally. Proper modeling of this phenomenon, normally neglected by conventional hypoelastic-plastic models, may have a significant effect on the accuracy of the model predictions of both laboratory test results and of solutions of boundary value problems.

This effect has been evaluated for undrained behavior of overconsolidated clays both in laboratory tests and in the tunnel excavation problem. In evaluation against experimental data, the proposed energy function allowed for accurate prediction of the deviation of effective undrained stress paths within the yield surface from the vertical straight lines predicted by isotropic hypoelastic models. This has a twofold effect on the solution of the BVP concerned with tunneling in undrained overconsolidated clay. At smaller stresses, within the yield surface, this deviation affects the solution directly, and when neglected may lead to underprediction of surface settlements. At larger stresses, when plastic flow dominates soil behavior, this deviation affects the solution indirectly, by setting different initial conditions for plastic yielding. In this case, when neglected, it may lead to the overprediction of surface settlements. It has also been shown that, for this particular problem, even significant variation in the parameters of the proposed energy function leads to smaller errors than those inflicted by neglecting energy conservation.

Acknowledgment

This research was supported by the Fund for the Promotion of Research at the Technion.

Notation

The following symbols are used in this paper:

C = isothermal compliance tensor;
D = isothermal stiffness tensor;
$d^g \geq 0$ = dissipation function;
f = helmholtz free energy function;
G' = shear modulus (according to Atkinson and Richardson 1985);
G^* = shear modulus (according to Graham and Houlsby 1983);
$\bar{G}$ = material constant in model defining shear modulus;
g = Gibbs free energy function;
J' = coupling modulus (according to Atkinson and Richardson 1985);
J^* = coupling modulus (according to Graham and Houlsby 1983);
J_0 = material constant in model, defining inherent cross-coupling;
K' = bulk modulus (according to Atkinson and Richardson 1985);
K^* = bulk modulus (according to Graham and Houlsby 1983);
$\bar{K}$ = material constant in model defining bulk modulus;
M = coefficient of friction ($q=Mp$ is failure criterion);
m = material constant defining bulk modulus power dependence on pressure;
n = material constant defining shear modulus power dependence on pressure;
p = mean effective stress;
p_{co} = initial intercept of yield surface on p axis;
p_r = reference pressure;
q = deviatoric stress;
ε_s = deviatoric strain;
ε_v = volumetric strain;
$\eta = q/p$ = stress ratio;
κ^* = elastic compressibility index;
λ = arbitrary non-negative multiplier; and
λ^* = compressibility soil index for virgin loading.

References

Addenbrooke, T. I., Potts, D. M., and Puzrin, A. M. (1997). ''The influence of pre-failure soil stiffness on the numerical analysis of tunnel construction.'' *Geotechnique*, 47(3), 693–712.

Atkinson, J. H. (2000). ''Non-linear soil stiffness in routine design.'' *Geotechnique*, 50(5), 487–508.

Atkinson, J. H., and Richardson, D. (1985). ''Elasticity and normality in soil—Experimental examinations.'' *Geotechnique*, 35(4), 443–449.

Borja, R. I., Tamagnini, C., and Amorosi, A. (1997). ''Coupling plasticity and energy-conserving elasticity models for clays.'' *J. Geotech. Geoenviron. Eng.*, 123(10), 948–957.

Boyce, H. R. (1980). ''A non-linear model for the elastic behaviour of granular materials under repeated loading.'' *Proc., Int. Symposium on Soils under Cyclic and Transient Loading*, January 7–11, Swansea, UK, 285–294.

Butterfield, R. (1979). ''A natural compression law for soils.'' *Geotechnique*, 29(4), 469–480.

Collins, I. F., and Houlsby, G. T. (1997). ''Application of thermomechanical principles to the modeling of geomaterials.'' *Proc. R. Soc. London, Ser. A*, 453, 1975–2001.

Einav, I. (2002). ''Applications of thermodynamical approaches to mechanics of soils.'' PhD dissertation, Technion-Israel Institute of Technology, Haifa, Israel.

Einav, I., and Puzrin, A. M. (2002). ''Discussion on 'Stress rate-elastic stretching relations in elastoplastic constitutive equations for soils' by K. Hashiguchi and I. F. Collins.'' *Soils Found.*, 42(1), 159–160.

Graham, J., and Houlsby, G. T. (1983). ''Anisotropic elasticity of a natural clay.'' *Geotechnique*, 33(2), 165–180.

Halphen, B., and Nguyen, Q. S. (1975). ''Sur les matériaux standards généralizés.'' *J. Mec.*, 14, 39–63.

Hardin, B. O. (1978). ''The nature of stress-strain behaviour for soils.'' *Proc., Geotechnical Division Special Conf. on Earthquake Engineering and Soil Dynamics*, ASCE, Pasdena, Calif., 1, 3–39.

Hashiguchi, K. (1995). ''On the linear relation of V-ln p and ln v-ln p for isotropic consolidation of soils.'' *Int. J. Numer. Analyt. Meth. Geomech.*, 19, 367–376.

Hashiguchi, K., and Collins, I. F. (2001). ''Stress rate-elastic stretching relations in elastoplastic constitutive equations for soils.'' *Soils Found.*, 41(2), 77–78.

Hoque, E., and Tatsuoka, F. (1998). ''Anisotropy in elastic deformation of granular materials.'' *Soils Found.*, 38(1), 163–179.

Houlsby, G. T. (1981). ''A study of plasticity theories and their applicability to soils.'' PhD thesis, Univ. of Cambridge, England.

Houlsby, G. T. (1985). ''The use of a variable shear modulus in elastic-plastic models for clays.'' *Comput. Geotech.*, 1, 3–13.

Houlsby, G. T., and Puzrin, A. M. (2000). ''A thermomechanical framework for constitutive models for rate-independent dissipative materials.'' *Int. J. Plast.*, 16(9), 1017–1047.

Houlsby, G. T., and Wroth, C. P. (1991). ''The variation of shear modulus of a clay with pressure and overconsolidation ratio.'' *Soils Found.*, 31(3), 138–143.

Hueckel, T., Tutumluer, E., and Pellegrini, R. (1992). ''A note on non-linear elasticity of isotropic overconsolidated clays.'' *Int. J. Numer. Analyt. Meth. Geomech.*, 16, 603–618.

ITASCA. (2000). *FLAC user's manual.*, Itasca Consulting Group Inc., Minneapolis.

Jovicic, V., and Coop, M. R. (1997). ''Stiffness of coarse-grained soils at small strains.'' *Geotechnique*, 47(3), 545–561.

Ko, H. Y., and Masson, R. (1976). ''Nonlinear characterization and analysis of sand.'' *2nd Int. Conf. on Numerical Methods in Geomechanics*,

C. S. Desai, ed., ASCE, Blacksburg, Va., 294–305.
Lee, K. M., and Rowe, R. K. (1989). ''Deformation caused by surface loading and tunneling: The role of elastic anisotropy.'' *Geotechnique*, 39(1), 125–140.
Lings, M. L., Pennington, D. S., and Nash, D. F. T. (2000). ''Anisotropic stiffness parameters and their measurement in a stiff natural clay.'' *Geotechnique*, 50(2), 109–125.
Lo Presti, D. C. F., and O'Neill, D. A. (1991). ''Laboratory investigation of small strain modulus anisotropy in sands.'' *Proc., ISOCCTI*, Clarkson Univ., Potsdam, N.Y., Huang, ed., Elsevier, New York, 213–224.
Love, A. E. H. (1927). *A treatise on the mathematical theory of elasticity*, Cambridge Univ., 4th Ed., Cambridge, England.
Maier, G., and Hueckel, T. (1977). ''Nonassociated and coupled flow rules of elastoplasticity for geomechanical media.'' *Proc., 9th Int. Conf. Soil Mechanics Foundation Engineering*, Tokyo, Specially session 7, Constitutive Relations for Soils, 129–142.
Martin, J. B., and Nappi, A. (1990). ''An internal variable formulation for perfectly plastic and linear hardening relations in plasticity.'' *Eur. J. Mech. A/Solids*, 9(2), 107–131.
Maugin, G. A. (1992). *The thermomechanics of plasticity and fracture*, Cambridge Univ., Cambridge, England.
Puzrin, A. M., and Houlsby, G. T. (2001a). ''A thermomechanical framework for rate-independent dissipative materials with internal functions.'' *Int. J. Plast.*, 17, 1147–1165.
Puzrin, A. M., and Houlsby, G. T. (2001b). ''Fundamentals of kinematic hardening hyperplasticity.'' *Int. J. Solids Struct.*, 38, 3771–3794.
Rampello, S., Viggiani, G. M. B., and Amorosi, A. (1997). ''Small-strain stiffness of reconstituted clay compressed along constant triaxial effective stress ratio paths.'' *Geotechnique*, 47(3), 475–489.
Stallebrass, S. E., and Taylor, R. N. (1997). ''The development and evaluation of a constitutive model for the prediction of ground movements in overconsolidated clay.'' *Geotechnique*, 47(2), 235–253.
Stokoe, K. H., II, Lee, J. N. K., and Lee, S. H. H. (1991). ''Characterization of soil in calibration chambers with seismic waves.'' *Proc., ISOCCTI*, Clarkson Univ., Potsdam, N.Y., Huang, ed., Vol. 2, Elsevier, New York, 363–376.
Truesdell, C. (1965). ''Hypo-elasticity.'' *J. Rational Mech. Anal.*, 4, 83–133.
Ziegler, H. (1977, 2nd Edition: 1983). *An introduction to thermomechanics*, North Holland, Amsterdam.
Zytynski, M., Randolph, M. F., Nova, R., and Wroth, C. P. (1978). ''On modelling the unloading-reloading behaviour of soils.'' *Int. J. Numer. Analyt. Meth. Geomech.*, 2, 87–93.